



# Photocatalytic oxidation mechanism of methanol and the other reactants in irradiated TiO<sub>2</sub> aqueous suspension investigated by OH radical detection

Jie Zhang, Yoshio Nosaka\*

Department of Materials Science and Technology, Nagaoka University of Technology, 1603-1 Kamitomioka, Nagaoka 940-2188, Japan

## ARTICLE INFO

### Article history:

Received 3 October 2014

Received in revised form 31 October 2014

Accepted 3 November 2014

Available online 15 November 2014

### Keywords:

Reaction mechanism

OH radical

TiO<sub>2</sub> photocatalysis

Methanol

Trapped holes

## ABSTRACT

The oxidation reaction mechanisms of organic additives, such as alcohols (MeOH and EtOH) and inorganic ions (I<sup>-</sup>, Br<sup>-</sup> and SCN<sup>-</sup>) in photocatalysis were elucidated by a fluorescence probe method by employing coumarin and coumarin-3-carboxylic acid as fluorescence probes. The general scheme of the oxidation and probing of OH radicals with coumarin was proposed. For the inorganic ions the photocatalytic oxidation was found to take place through OH radicals while for the organic molecules the oxidation should proceed by the exertion of the holes trapped on the TiO<sub>2</sub> surface. This is supported by the fact that the quantum efficiency of the CO<sub>2</sub> formation by MeOH oxidation was about ten times larger than that of the OH radical formation. The OH radicals in solution are most probably in equilibrium with the trapped holes, and the equilibrium constant could be estimated to be about 0.014 by assuming the diffusion controlled reaction of MeOH with trapped holes.

© 2014 Elsevier B.V. All rights reserved.

## 1. Introduction

Since Fujishima and Honda discovered photo induced water cleavage by TiO<sub>2</sub> [1], titanium dioxide has been attracting much attention due to its low toxicity, low cost, high thermal and chemical stability. Owing to the intensive studies by many researchers, it has been widely used for environmental applications, such as water treatment, air purification, and soil remediation [2–5]. On photo excitation, several active oxygen species such as OH radical ( $\cdot$ OH), superoxide radical ( $\cdot$ O<sub>2</sub><sup>-</sup>), and H<sub>2</sub>O<sub>2</sub> were formed by the reactions with generated electrons and holes. Among them,  $\cdot$ OH seems considerably important because it has been frequently recognized as the major reactant responsible for the photocatalytic oxidization of organic compounds [2].

Methanol is widely used in photocatalytic studies on TiO<sub>2</sub> [6,7], and the photocatalysis on TiO<sub>2</sub> is important especially in environmental cleaning. It has been inferred that  $\cdot$ OH is responsible for the oxidation pathways of organic compounds initiated by heterogeneous photocatalytic processes. Some research groups used methanol as a scavenger to investigate the generation of  $\cdot$ OH on the surface of TiO<sub>2</sub> in the photocatalytic reaction [8]. However, many

of the other researchers were suspicious about the involvement of  $\cdot$ OH in the oxidization of methanol. For example, Yung et al. [9] used methanol as a hole scavenger on the contrary. Furthermore, by highly sensitive femtosecond and nanosecond spectroscopy, Tamaki et al. [10] observed the absorption of trapped holes formed in nanocrystalline TiO<sub>2</sub> films and reported that oxidation reactions of some kinds of alcohols could be regarded as electron transfer from alcohols to adjacent surface holes. In aqueous solutions, a competitive reaction would take place between the direct oxidation of organic molecules and the indirect oxidation through OH radicals which are formed from water by holes [6]. Concerning the MeOH oxidization, it remains unclear whether the molecules are oxidized through the direct interfacial transfer of photo-generated holes or the step reaction with photo-generated hydroxyl radicals [7].

The detection of OH radicals is not feasible due to its high reactivity and short life time. Recently, we have reported that a fluorescence probe method with terephthalic acid (TA) is a suitable method to detect  $\cdot$ OH in photocatalysis in aqueous suspension [11–13]. Furthermore, by employing coumarin (Cou) as a fluorescence probe, we have proposed the reaction mechanisms of visible-light responsive photocatalysts by analyzing OH radicals quantitatively [14]. Then, mechanisms of the OH radical generation in TiO<sub>2</sub> with different crystalline types were explored [15]. By using TA, Ahmed et al. [6] reported the higher activity of the

\* Corresponding author. Tel.: +81 258 47 9315; fax: +81 258 47 9315.

E-mail address: nosaka@nagaokaut.ac.jp (Y. Nosaka).

photocatalytic MeOH decomposition on the anatase single crystallites as compared to rutile single crystallites, despite the fact that both show the same OH radical generation.

In the present study, in order to clarify the photocatalytic oxidation mechanism of MeOH, the effect of the additives on the OH radical generation was investigated. Besides coumarin, coumarin-3-carboxy acid (CCA) was employed as a fluorescence probe to investigate the location dependence of the OH radical probe, which provided valuable information about the behavior of OH radical near the TiO<sub>2</sub> surface [15]. In order to compare the reaction mechanisms for organic molecules with those for inorganic molecules, the oxidations of inorganic ions such as I<sup>-</sup>, Br<sup>-</sup> and SCN<sup>-</sup> were also investigated. Based on the observed rate constants for the reaction of the additives with the photo generated OH radicals, the oxidation mechanism of MeOH was discussed along with the relationship between trapped holes and OH radicals.

## 2. Experimental

### 2.1. Materials

The TiO<sub>2</sub> powders, ST-01 (Ishihara Sangyo Co.), MT-150A (TAYCA Co.), and P25 (Nippon Aerosil Co.), were generous gifts from each manufacturer and used without modification. The composition of crystalline phase, particle size, and BET surface area were listed in Table 1. The other properties such as point of zero charges of these samples have been listed in the previous reports [15].

Coumarin (Cou) and 7-hydroxy coumarin (OH-Cou, umbelliferone) (Tokyo Kasei Co.), and coumarin-3-carboxylic acid (CCA) and 7-hydroxy-coumarin-3-carboxylic acid (OH-CCA) (Sigma-Aldrich Co.), and potassium chloride, potassium iodide, potassium bromide, potassium thiocyanate, methanol (MeOH), and ethanol (EtOH) (Nacalai Tesque Co.) were used without further purification.

### 2.2. Detection of OH Radicals

Previously, we used terephthalic acid (TA) as a probe molecule for •OH detection in alkaline solution [11–13]. Recently we have been employing coumarin [14] and coumarin-3-carboxylic acid (CCA) [15] for the detection of •OH instead for some reasons. Coumarin carries no charge and is not adsorbed on the surface of TiO<sub>2</sub> but can detect •OH in TiO<sub>2</sub> suspension. On the other hand, CCA possesses a -COOH group which adsorbs at the terminal OH of TiO<sub>2</sub>, and can detect •OH near the TiO<sub>2</sub> surface [15].

Experimental procedure of the fluorescence probe method was described in detail elsewhere [14]. Briefly, 3.5 mL of a 0.1 mM CCA or coumarin aqueous solution with different concentration of additives was added in a Pyrex cell (10 mm × 10 mm × 45 mm), then TiO<sub>2</sub> powder (15 mg) was suspended in the solution in dark. The additives were KI, KBr, KSCN, MeOH and EtOH. When one of the additives was added, in order to attain the adsorption equilibrium between TiO<sub>2</sub> and the additive, the suspension was kept in dark for 1 h before irradiation. One side of the cell was irradiated with UV light emitted from an LED lamp (365 nm, Nichia, NCCU033) through a quartz convex lens. The light intensity was measured with a power meter (Advantest, TQ8210) and the excitation rate was calculated from the reflection spectra as described previously [15].

The suspension was stirred vigorously for 5 min before and during the light irradiation. After the irradiation for a given time (150 s), 0.5 g of KCl was added into the suspension, and then the suspension was kept in dark to precipitate the powder. After 1 day holding, the clear solution was obtained and its fluorescence spectrum was measured with the excitation wavelength of 340 or 332 nm for OH-CCA or OH-coumarin, respectively. Fluorescence spectra

were measured with a fluorescence spectrophotometer (Hitachi, Model 850) equipped with a PC recorder. The intensity of the each spectrum could be corrected by the fluorescence peak of CCA or coumarin at 390 or 392 nm, respectively. For the experiment with 0.5 mM coumarin, fluorescence spectra were measured after dilution to one fifth. In the separate experiments, we had confirmed that KCl did not affect the fluorescence intensities.

### 2.3. Calculation of •OH concentration

The amount of •OH was calculated from the concentration of OH-CCA with the conversion factor,  $\alpha$ , obtained by the following derivation with some references. On the irradiation of a  $\gamma$ -ray in 0.1 mM coumarin aqueous solution, several OH substitutes of coumarin are produced due to the reaction with •OH [16]. Among the products, only 7-OH substitute coumarin (OH-coumarin) emits strong fluorescence and the yield is reported to be 14 nmol/J for 0.1 mM coumarin [16]. For 1 mM coumarin, it slightly increased to 16 nmol/J, suggesting the reaction with coumarin is the dominant process of •OH deactivation. The yield of •OH on the  $\gamma$ -ray irradiation in pure water is reported to be 2.2 molecules/100 eV [17], which corresponds to 228 nmol/J. On the basis of the comparison of the yields of OH-Cou with •OH, it is calculated that 6.1% of •OH in water can be probed as OH-coumarin by using 0.1 mM coumarin. For 0.1 mM CCA, 4.7% of OH radicals can be probed by the formation of OH-CCA [18], where the total concentration of OH-CCA was calculated by taking account of the fraction of adsorbed OH-CCA which could not be detected.

### 2.4. Adsorption of organic molecules

Adsorption of MeOH and EtOH on each TiO<sub>2</sub> powder was examined by the fraction of non-adsorbed probe molecule as follows. TiO<sub>2</sub> powder (30 mg) was added to 7 mL of 0.1 mM CCA aqueous solutions containing 50 nM OH-CCA and various amounts of the alcohol (MeOH or EtOH). The solution was vigorously stirred and placed for 1 h for adsorption. Then, into the solution, 1 g of KCl was added and kept in the dark for 1 day to measure the fluorescence spectra of the supernatant solution.

### 2.5. Detection of CO<sub>2</sub>

The decompositions of MeOH and EtOH in TiO<sub>2</sub> aqueous suspension were examined by monitoring the amount of the final product, CO<sub>2</sub>. The concentration of CO<sub>2</sub> during the reaction was measured with an ion meter (TOA, IM-32P) with a CO<sub>2</sub> electrode (TOA, CE2041). The experimental procedure was as follows. Photocatalyst suspension was prepared by adding photocatalyst powder (150 mg) into 35 mL of purified water in a 50 mL glass bottle. This suspension was sonicated for 5 min and stirred vigorously for 1 h under ambient condition to attain an equilibratory CO<sub>2</sub> condition. Then, the diluted organic solution was added into this suspension in dark and the CO<sub>2</sub> electrode was immersed into the suspension. The suspension was sealed with a silicon cap so as to occupy fully the bottle without space of air. The irradiation source was the same as the other experiments in the research. The suspension was stirred vigorously during the irradiation. The formation rate of CO<sub>2</sub> was calculated from the increase of the CO<sub>2</sub> concentration with the irradiation time up to 30 min. The initial concentrations of CO<sub>2</sub> and O<sub>2</sub> are estimated to be 0.5 and 8 ppm, respectively. Although the dissolved O<sub>2</sub> in the sealed mixture would be consumed during the oxidation, the decrease of the O<sub>2</sub> concentration can be ignored for the detection of initial decomposition of organic molecules with forming of CO<sub>2</sub> up to 0.3 ppm.

**Table 1**

Photo absorption rate, •OH generation rate (g) measured with coumarin and CCA, and CO<sub>2</sub> formation rate with decomposition of methanol and ethanol for various TiO<sub>2</sub>.

| Name of TiO <sub>2</sub> | Composition | Photo absorption rate/ $10^{-5}$ M s <sup>-1</sup> | Particle size/nm<br>[19] | BET surface area/m <sup>2</sup> g <sup>-1</sup> | g/10 <sup>-9</sup> M s <sup>-1</sup> |      | CO <sub>2</sub> generation rate/ $10^{-3}$ ppm min <sup>-1</sup> |      |
|--------------------------|-------------|--|--------------------------|---|--------------------------------------|------|--|------|
|                          |             |  |                          |   | Cou                                  | CCA  | MeOH   | EtOH |
| ST-01                    | 100% A      | 1.0  | 7                        | 320   | 1.8                                  | 7.2  | 2.4  | 1.1  |
| P25                      | 80% A       | 1.1  | 32                       | 49  | 2.5                                  | 30.8 | 24   | 3.4  |
| MT-150A                  | 100% R      | 1.3  | 15                       | 88  | 0.12                                 | 0.47 | 0.0  | 0.0  |

### 3. Basic kinetic analysis

Competitive reactions for •OH with coumarin and an additive A, such as MeOH could be represented as follows. The •OH is generated by the photo excitation (Eq. (1)), then it could react with both the probe coumarin (Cou) (Eq. (2)), and the additive A (Eq. (3)). Where,  $g$  in Eq. (1) represents the generation rate of •OH,  $k_c$  and  $k_A$  are second order reaction constants,  $\alpha$  in Eq. (2) represents the fraction of the fluorescent molecule of the products. For OH-coumarin (OH-Cou),  $k_c = 1.3 \times 10^9 \text{ M}^{-1} \text{ s}^{-1}$  [15], and  $\alpha = 0.061$  as described above.



On the basis of the steady state approximation for •OH (Eqs. (4) and (5)), formation rate of OH-coumarin could be expressed by Eq. (6). Since the rate of the formation was constant, the concentration of OH-coumarin at time  $t$ , which is denoted by  $[\text{OH-Cou}]_t$ , is proportional to  $t$ . Then, the reciprocal number of  $[\text{OH-Cou}]_t$  can be expressed as a function of the concentration of additives [A] as shown in Eq. (7). Therefore, the slope of the  $1/[\text{OH-Cou}]_t - [\text{A}]$  plot provides the reaction rate constant of A with OH radicals.

$$\frac{d[\cdot\text{OH}]}{dt} = g - k_c [\cdot\text{OH}] [\text{Cou}] - k_A [\cdot\text{OH}] [\text{A}] \quad (4)$$

$$[\cdot\text{OH}] = \frac{g}{k_c [\text{Cou}] + k_A [\text{A}]} \quad (5)$$

$$\frac{d[\text{OH-Cou}]}{dt} = \alpha \cdot k_c [\cdot\text{OH}] [\text{Cou}] = \frac{g \alpha k_c [\text{Cou}]}{k_c [\text{Cou}] + k_A [\text{A}]} \quad (6)$$

$$\frac{1}{[\text{OH-Cou}]_t} = \frac{1}{t \cdot g \cdot \alpha} + \frac{k_A}{t \cdot g \cdot \alpha \cdot k_c \cdot [\text{Cou}]} \cdot [\text{A}] \quad (7)$$

Eq. (7) is equivalent to that used in the previous report [15], in which the addition of I<sup>-</sup> was analyzed. Thus, the value of  $t \cdot g \cdot \alpha$  in Eq. (7) is equal to  $[\text{OH-Cou}]_t$  observed in the absence of the additive.

When CCA was used as a fluorescence probe in place of coumarin, the probing reaction, Eq. (2), becomes Eq. (8).



The same series of equations from (3) to (7) can be drawn by replacing [Cou] and [OH-Cou] by [CCA] and [OH-CCA], respectively. In this case,  $k_c$  and  $\alpha$  should be  $2.7 \times 10^8 \text{ M}^{-1} \text{ s}^{-1}$  and 0.047, respectively [15].

## 4. Results

### 4.1. Photocatalytic oxidation of MeOH and EtOH

Before the estimation of OH radical production, for comparison, the catalytic activity of the TiO<sub>2</sub> used has been estimated by the decomposition of MeOH and EtOH. Fig. 1(a) and (b) shows the generation of CO<sub>2</sub> during the photocatalytic oxidation of MeOH and EtOH, respectively. From the slope the generation rate of CO<sub>2</sub> was calculated and listed in Table 1. No generation of CO<sub>2</sub> was observed

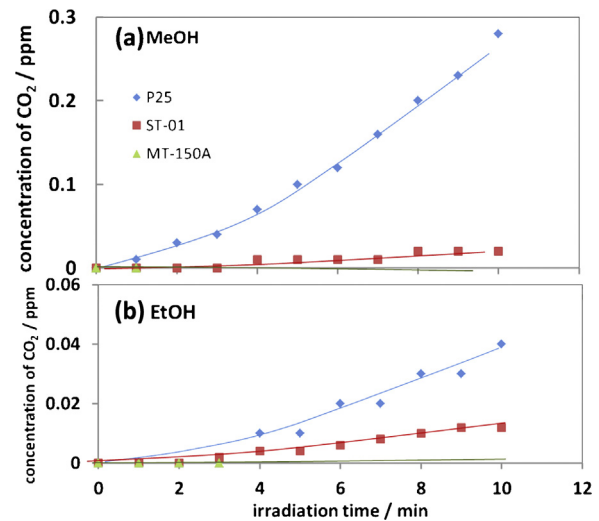


Fig. 1. Generation of CO<sub>2</sub> by photocatalytic oxidation of (a) MeOH and (b) EtOH by three kinds of TiO<sub>2</sub> (P25, ST-01 and MT-150A).

for rutile TiO<sub>2</sub>. The generation rate of CO<sub>2</sub> for P25 TiO<sub>2</sub> was much larger than that for ST-01. The oxidation rate of MeOH (a) was larger than that of EtOH (b) for both P25 and ST-01. However, it is noted that the difference in the oxidation rates of MeOH and EtOH is much larger for P25 TiO<sub>2</sub> than for ST-01, suggesting the different oxidation reaction process for P25 and pure anatase TiO<sub>2</sub> (ST-01).

### 4.2. Adsorption of EtOH and MeOH

Fig. 2 shows the fluorescence spectra of 50 nM OH-CCA in 0.1 mM CCA with and without MeOH or EtOH. Fluorescence peaks for OH-CCA and CCA were observed at 443 nm and 390 nm, respectively. Fig. 2(a) shows the fluorescence spectra of the solution after the adsorption with MT-150A and P25 TiO<sub>2</sub> powders, on which 24% and 97% of OH-CCA are adsorbed, respectively [15]. As shown in Fig. 2(a), the fluorescence spectra scarcely changed with EtOH, neither with MeOH (spectra were not shown). These observations suggest that, even if alcohols were adsorbed on the TiO<sub>2</sub> surface, the adsorption of OH-CCA should be stronger than that of the alcohols. On the other hand, as shown in Fig. 2(b) in the case of ST-01 TiO<sub>2</sub>, the fluorescence intensity of OH-CCA increased with the addition of MeOH and EtOH, indicating that alcohols could be adsorbed on the surface of ST-01 with the desorption of OH-CCA. Since the amount of released OH-CCA for 2.8 mM MeOH is smaller than that for 2.7 mM EtOH, the adsorption of EtOH is slightly stronger than that of MeOH.

### 4.3. Reaction of •OH with additives

At first, the effect of the coumarin concentration on the reaction rate of •OH formation was examined. For 0.1 and 0.5 mM coumarin, the plot of  $1/[\text{OH-Cou}]_t$  against the concentration of MeOH is shown in Fig. 3. Without MeOH, the formation rate did not change significantly with the increase of the coumarin concentration. On the

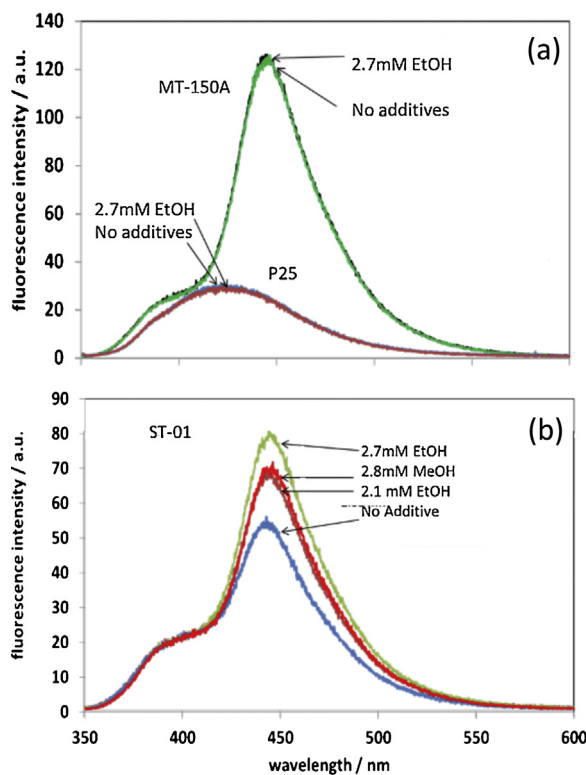


**Fig. 2.** Effect of MeOH and EtOH on the adsorption of OH-CCA at the surface of (a) MT-150A, P25, and (b) ST-01  $\text{TiO}_2$ .

addition of MeOH, the slope for 0.5 mM coumarin became about one tenth of that for 0.1 mM. This observation is consistent with the Eq. (7) which was derived from the reaction of MeOH with OH radicals, although there might be some experimental errors in the evaluation of the slope.

Then, to elucidate the photocatalytic reaction of alcohols and halide ions, we performed a series of experiments for five additives ( $\text{SCN}^-$ ,  $\text{Br}^-$ ,  $\text{I}^-$ , MeOH, and EtOH) and three kinds of  $\text{TiO}_2$  (P25, ST-01, and MT-150A) by using two fluorescent probes (coumarin and CCA). In this accurate experiments, the light source was confined with the  $8\text{mm} \times 8\text{mm}$  aperture, and the photo excitation rates for each  $\text{TiO}_2$  were measured and listed in Table 1. Averaged value of  $g$  measured without additives are also shown in Table 1. From the plot against the concentration of additives,  $k_A$  was calculated based on Eq. (7) with the value of  $g$  and shown in Table 2. For the reason that OH radicals were produced by three electron oxidation of water on rutile  $\text{TiO}_2$  [20], the amount of generated OH radicals by MT-150A

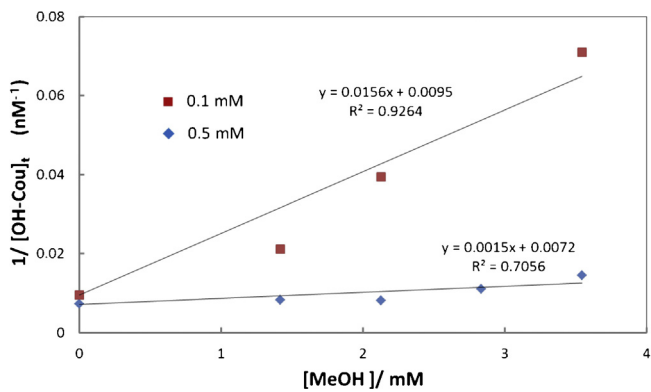


**Fig. 3.** The plot of  $1/[\text{OH-Cou}]_t$  against the concentration of MeOH with different concentration of probes (0.1 and 0.5 mM coumarin).

**Table 2**

The reaction rate of OH radicals with some additives elucidated from the concentration dependence of  ${}^\bullet\text{OH}$  formation rate measured with fluorescence probe molecules coumarin (Cou) and coumarin-3-carboxylic acid (CCA).

| $\text{TiO}_2/\text{probe}$ | $k_A/10^9 \text{ M}^{-1} \text{ s}^{-1}$                |               |              |        |         |
|-----------------------------|---|---------------|--------------|--------|---------|
|                             | $\text{SCN}^-$  | $\text{Br}^-$ | $\text{I}^-$ | MeOH   | EtOH    |
| ST-01                       |   |               |              |        |         |
|                             | Cou   | 0.40          | 2.16         | 0.75   | 0.21    |
| P25                         | CCA   | 0.10          | 0.37         | 0.37   | 0.0068  |
|                             | Cou   | 15.2          | 16.9         | 10.5   | 0.14    |
| MT-150A                     | CCA   | 8.62          | 3.52         | 0.95   | 0.00052 |
|                             | Cou   | —             | —            | 0.039  | —       |
|                             | CCA   | —             | —            | 0.0061 | 0.016   |
|                             | $k_{\text{OH}}/10^9 \text{ M}^{-1} \text{ s}^{-1}$ [21] | 11            | 11           | 11     | 1.9     |

was small as shown by  $g$  in Table 1. Then,  $k_A$  could not be calculated and the corresponding cells in Table 2 were left blank. The reaction rates in homogeneous aqueous solution  $k_{\text{OH}}$  in the literature [21] are also listed in Table 2.

## 5. Discussion

Since the wavelength of the excitation light was 365 nm, the photo absorption rate did not change much between rutile and anatase as shown in Table 1. The generation rate of OH radical measured with coumarin and CCA was compared with that of the  $\text{CO}_2$  in Fig. 4, where the  $\text{CO}_2$  generation rate was calculated by taking account of the difference in the reaction volume. As shown in Fig. 4 (right half),  $\text{CO}_2$  formation by the photocatalytic decomposition of both alcohols for mixed crystalline P25  $\text{TiO}_2$  was larger than pure anatase ST-01  $\text{TiO}_2$ , which means a stronger oxidation ability of P25. And this is also in accord with that the generation rate of OH radicals for P25 is larger than that for ST-01 (left half). On the other hand, the oxidation rate of MeOH was larger than that of EtOH, which was not in accord with the reaction rate of OH radicals shown in Table 2, neither the adsorption ability in Fig. 2(b). The  ${}^\bullet\text{OH}$  generation rate measured with CCA for P25  $\text{TiO}_2$  was three times larger than that of  $\text{CO}_2$ . However, since 4-electrons are removed from MeOH to produce one  $\text{CO}_2$  molecule, the oxidation rate of MeOH is calculated to be  $3.6 \times 10^{-7} \text{ M s}^{-1}$ . By divided it with the photo adsorption rate in Table 1, the quantum efficiency of the oxidation is calculated to be 3%. On the other hand, the quantum efficiency of  ${}^\bullet\text{OH}$  production measured with CCA is 0.28% ( $30.8 \times 10^{-9} \text{ M s}^{-1}/1.1 \times 10^{-5} \text{ M s}^{-1}$ ). Since the  ${}^\bullet\text{OH}$  formation was one tenth of the oxidation, MeOH must not be oxidized with OH radicals.

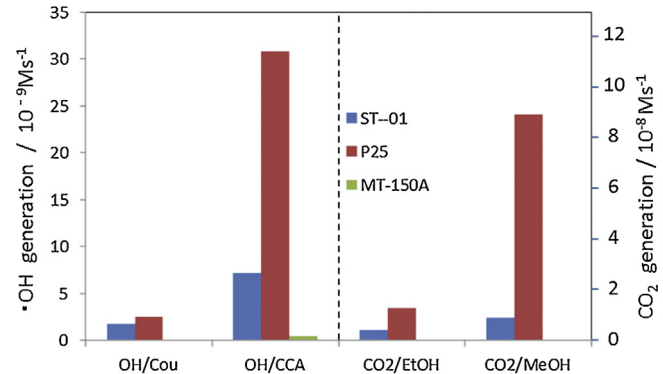


**Fig. 4.** OH radical generation rate measured by Cou and CCA probe (left half) and the  $\text{CO}_2$  formation rate by the decomposition of EtOH and MeOH (right) with ST-01, P25, and MT-150A  $\text{TiO}_2$  powders.

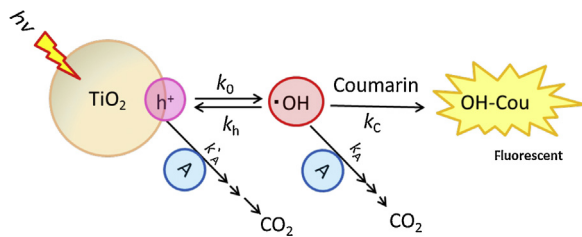


**Fig. 5.** A general scheme for the OH radical detection by a fluorescence probe method in the oxidation process of reactant A.

The value  $k_A$  in Table 2 was evaluated by the competitive reaction of probe molecules, Cou and CCA, with several kinds of additives, A. However, the values of  $k_A$  measured with CCA were smaller than those with Cou for all additives. This difference originated from the decrease in the effective CCA concentration due to the adsorption of CCA [15]. Besides,  $k_A$  for SCN<sup>-</sup>, I<sup>-</sup>, and Br<sup>-</sup> are closed to the reported rate constants,  $k_{\text{OH}}$ , whereas it was significantly smaller for alcohols. This observation indicates that OH radicals react with inorganic ions, but the reaction with alcohols hardly occurs.

Thus, for the kinetic analysis of alcohol oxidation, we should adopt the direct oxidation by trapped holes but not by OH radicals. Then, we modified the equations in the basic kinetic analysis to involve the oxidation by photogenerated holes, or trapped holes of TiO<sub>2</sub>. The holes  $\text{h}^+$  are generated by the photo absorption (Eq. (1'a)), followed by the oxidation of A (Eq. (3')) with the reaction rate constant of  $k'_A$ . In this case, the generated  $\text{h}^+$  produces •OH (Eq. (1'b)), which reacts with probe molecules. Total scheme is shown in Fig. 5. Here, coumarin would not be oxidized to OH-Cou by holes, because the concentration dependence of coumarin on the formation of OH-Cou was not observed (Fig. 3).



The kinetic analysis similar to the basic analysis of the series of equations from (1) to (7) can be applied. By replacing Eqs. (1) and (3) with Eqs. (1'a), (1'b), and (3'), and adopting steady-state approximation for  $\text{h}^+$ , Eq. (7b) can be obtained for the  $1/[\text{OH-Cou}]_t - [\text{A}]$  plot.

$$\frac{1}{[\text{OH-Cou}]_t} = \frac{1}{t \cdot g' \cdot \alpha} + \frac{k'_A}{t \cdot g' \cdot \alpha \cdot k_0} \cdot [\text{A}] \quad (7b)$$

However, as shown in Fig. 3, the slope of the  $1/[\text{OH-Cou}]_t - [\text{A}]$  plot depended on the concentration of coumarin, [Cou]. To solve this discrepancy, we should take into account the reverse reaction of Eq. (1'b), that is the adsorption of •OH to form trapped holes. The presence of the equilibrium between •OH and trapped holes have been suggested in the previous study [14].



By taking Eq. (1'c) into account of the kinetic analysis, Eq. (7b) becomes Eq. (7c).

$$\frac{1}{[\text{OH-Cou}]_t} = \frac{k_0}{t \cdot g' \cdot \alpha} + \frac{k'_A(k_h + k_c[\text{Cou}])}{t \cdot g' \cdot \alpha \cdot k_c[\text{Cou}]} \cdot [\text{A}] \quad (7c)$$

Since the slope of the  $1/[\text{OH-Cou}]_t - [\text{A}]$  plot was decreased with the increase of [Cou], the value of  $k_h$  should be larger than  $k_c[\text{Cou}] (=1.3 \times 10^9 \text{ M}^{-1} \text{ s}^{-1} \times 5 \times 10^{-4} \text{ M} = 6.5 \times 10^5 \text{ s}^{-1})$ . In this case, the comparison of Eq. (7c) with Eq. (7), leads to that  $g'$  and

$k'_A$  corespond to  $gk_0$  and  $k_A k_0/k_h$ , respectively. The latter relation is equivalent to  $k_0/k_h = k'_A/k_A$ . When  $k'_A$  is assumed to be the diffusion controlled rate constant ( $1 \times 10^{10} \text{ M}^{-1} \text{ s}^{-1}$ ),  $k_0/k_h$  which corresponds to the equilibrium constant becomes 0.014, because  $k_A = 0.14 \times 10^9 \text{ M}^{-1} \text{ s}^{-1}$  for MeOH with P25 TiO<sub>2</sub> and coumarin. Then, the value of  $k_0$  could be estimated to be  $k_0 = k_h k'_A/k_A > 9 \times 10^4 \text{ s}^{-1}$  ( $=6.5 \times 10^5 \text{ s}^{-1} \times 0.14 \times 10^9 \text{ M}^{-1} \text{ s}^{-1}/1 \times 10^{10} \text{ M}^{-1} \text{ s}^{-1}$ ). In this estimation,  $k_A$  for CCA could not be applied because the concentration of CCA effective to the reaction with •OH could not be correctly evaluated due to the adsorption on the TiO<sub>2</sub> surface.

## 6. Conclusion

The oxidation reaction mechanisms of organic additives, such as alcohols (MeOH and EtOH) and inorganic ions (I<sup>-</sup>, Br<sup>-</sup> and SCN<sup>-</sup>) in photocatalysis were elucidated by a fluorescence probe method by employing coumarin and coumarin-3-carboxylic acid as fluorescence probes. For the inorganic ions the photocatalytic oxidation was found to take place through OH radicals. On the other hand, interestingly, for the organic molecules it was suggested that the oxidation should not take place by the OH radicals but by the holes trapped on the TiO<sub>2</sub> surface. This is supported by the fact that the quantum efficiency of the CO<sub>2</sub> formation by MeOH oxidation was 10 times larger than that of the OH radical formation. The general scheme of the oxidation and probing of OH radicals with coumarin is summarized in Fig. 5. Based on the kinetic analysis of the concentration dependence for the coumarin probe, the photogenerated OH radicals in solution are most probably in equilibrium with the holes trapped on the TiO<sub>2</sub> surface. By assuming the diffusion controlled reaction of MeOH with  $\text{h}^+$ , the equilibrium constant could be estimated to be  $k_0/k_h = 0.01$ .

## Acknowledgement

We thank Dr. Atsuko Y. Nosaka for the valuable comments on the manuscript preparation.

## References

- [1] A. Fujishima, K. Honda, Nature 238 (1972) 37–38.
- [2] M.R. Hoffmann, S.T. Martin, W. Choi, D.W. Bahnemann, Chem. Rev. 95 (1995) 69–96.
- [3] A. Fujishima, X. Zhang, D. Tryk, Surf. Sci. Rep. 63 (2008) 515–582.
- [4] M. Anpo, P.V. Kamat (Eds.), Environmentally Benign Photocatalysts – Applications of Titanium Oxide-based Materials, Springer Publishers, Inc., New York, Dordrecht, Heidelberg, London, 2010.
- [5] P. Pichat (Ed.), Photocatalysis and Water Purification, Wiley-VCH, Manheim, Germany, 2013.
- [6] A.Y. Ahmed, T.A. Kandiel, T. Oekermann, D. Bahnemann, J. Phys. Chem. Lett. 2 (2011) 2461–2465.
- [7] A.Y. Ahmed, T.A. Kandiel, I. Ivanova, D. Bahnemann, Appl. Surf. Sci. 319 (2014) 44–49.
- [8] Y. Du, J. Rabani, J. Phys. Chem. B 107 (2003) 11970–11978.
- [9] Y.K. Kho, A. Iwase, W.Y. Teoh, L. Madler, A. Kudo, R. Amal, J. Phys. Chem. C 114 (2010) 2821–2829.
- [10] Y. Tamaki, A. Furube, M. Murai, K. Hara, R. Katoh, M. Tachiya, J. Am. Chem. Soc. 128 (2006) 416–417.
- [11] T. Hirakawa, Y. Nosaka, Langmuir 18 (2002) 3247–3254.
- [12] Y. Nosaka, S. Komori, K. Yawata, T. Hirakawa, A. Nosaka, Phys. Chem. Chem. Phys. 5 (2003) 4731–4735.
- [13] T. Hirakawa, K. Yawata, Y. Nosaka, Appl. Catal. A 325 (2007) 105–111.
- [14] J. Zhang, Y. Nosaka, J. Phys. Chem. C 117 (2013) 1383–1391.
- [15] J. Zhang, Y. Nosaka, J. Phys. Chem. C 118 (2014) 10824–10832.
- [16] G. Louit, S. Foley, J. Cabillac, H. Coffigny, F. Taran, A. Valleix, J.P. Renault, S. Pin, Radiat. Phys. Chem. 72 (2005) 119–124.
- [17] F.S. Dainton, W.S. Watt, Nature 195 (1962) 1294–1296.
- [18] L.N. Gerald, R.M. Jamie, Radiat. Phys. Chem. 75 (2006) 473–478.
- [19] Y. Murakami, J. Nishino, T. Mesaki, Y. Nosaka, Spectrosc. Lett. 44 (2011) 88–94.
- [20] Y. Nakabayashi, Y. Nosaka, J. Phys. Chem. C 117 (2013) 23832–23839.
- [21] G.V. Buxton, C.L. Greenstock, W.P. Helman, A.B. Ross, J. Phys. Chem. Ref. Data 17 (1988) 513–886.